AAS 18-054

FUEL-OPTIMAL AND APOLLO POWERED DESCENT GUIDANCE COMPARED FOR HIGH-MASS MARS MISSION

Ping Lu*

A human Mars mission will necessitate a significantly higher landing mass and landing precision than in any robotic missions ever attempted so far. The need for all-propulsive descent and landing for such a high-mass entry, descent, and landing (EDL) mission further increases the propellant mass fraction. The propellant usage required by the powered descent guidance algorithm can have a huge implication on the mission. In this work we set out to gain an understanding of how the propellant performance compares between an advanced fuel-optimal powered descent guidance algorithm and the venerable Apollo powered descent guidance in a high-mass Mars EDL mission. It is revealed that the powered descent initiation (PDI) condition for, and the time-to-go used in, the Apollo guidance affect greatly the propellant usage, under otherwise the same condition. Yet there has been thus far a lack of systematic and effective approaches to *autonomously* determine favorable PDI condition and time-to-go for ensured landing and good propellant performance of the Apollo guidance. In this paper a method is developed that makes use of a capability of a most recent fuel-optimal powered descent guidance algorithm to determine online a best PDI condition and the corresponding time-to-go for the Apollo guidance, based on the actual flight condition. It is shown that with this adaptive PDI logic the Apollo powered descent guidance can achieve a propellant performance that is very close to the optimal propellant consumption for a high-mass Mars EDL mission, while maintaining high landing precision.

INTRODUCTION

A human Mars mission would require a landing mass at least an order of magnitude more than the heaviest robotic rover ever landed on Mars. Furthermore, all-propulsive descent and landing by a supersonic retropropulsion (SRP) system would be necessary for such a high-mass vehicle. Desirable landing accuracy is expected to be on the order of 50 meters. Without sacrificing the safety and precision, the reduction of every kilogram of propellant usage during the entry, descent, and landing (EDL) will have a nontrivial implication up stream, all the way to launch at Earth. Propellant consumption of the SRP is greatly affected by the powered guidance algorithm. A propellant-optimal (or fuel-optimal) powered descent guidance algorithm, called Universal Powered Guidance (UPG), was recently developed with human Mars or lunar missions in mind. [1] This algorithm is fast and still relatively simple. With the strong capability of UPG to find quickly the fuel-optimal powered descent and landing trajectory from the powered descent initiation (PDI) point to touchdown, Ref. [2] offers an evaluation of the performance of UPG in a human Mars mission. Moreover, it is demonstrated in Ref. [2] how a numerical predictor-corrector entry guidance algorithm and UPG can be integrated together to bring significant propellant usage reduction in a human Mars mission.

The classical Apollo Lunar Descent Guidance (ALDG) [3, 4] is flight proven, and it has been the baseline powered descent guidance method for many robotic planetary missions since the Apollo Program. Any new powered descent guidance algorithm should demonstrate its worthiness against ALDG. The ALDG law based on a quadratic thrust acceleration profile is very simple. However, it is not fuel optimal. For a human Mars mission, it is very useful to understand what is the optimal propellant consumption, and how the propellant usage by the ALDG compares to the best possible value for the same mission. In this paper, we go one step

*Professor and Chair, Department of Aerospace Engineering, San Diego State University, San Diego, CA 92182, plu@sdsu.edu

further in developing a method that significantly enhances the propellant performance of Apollo powered descent guidance by augmenting it with a capability of the UPG.

In the process of evaluating the propellant performance of the ALDG for a human Mars mission, it is found that its performance in propellant consumption and guidance precision are very much dependent on the selection of the powered descent initiation (PDI) condition and the time-to-go used in the ALDG law. Along the entry trajectory, the closer the PDI is to the landing site, and the shorter the time-to-go is, the less propellant consumption is for ALDG. However, since the ALDG law does not explicitly take the thrust magnitude bounds into consideration, pressing too hard on the PDI condition and time-to-go will result in thrust saturation, thus large errors in the landing condition (in both position and velocity). These findings are likely known to those who have used ALDG in Mars applications in one form or another, even though they may not have been widely reported. What has not been available, at least in open literature, is a systematic, effective, and automated method to make determination of the desirable PDI condition and time-to-go.

The two main goals of this paper are to

1. Provide a side-by-side simulation study of UPG and ALDG in a human Mars mission to establish a benchmark of propellant consumption comparison

2. Improve the performance of ALDG by addressing the aforementioned two long-standing challenges in applying ALDG that decidedly affect the landing precision and propellant consumption of ALDG

Toward these ends, we will first provide an overview of the basics of UPG for the convenience of the reader. [1] The integration of the entry guidance and UPG in the EDL mission is also reviewed. [2] Closed-loop Monte Carlo simulations with a mid lift-to-drag rigid-body vehicle (MRV) concept [5] from entry interface (EI) to touchdown for a human Mars mission are carried out, using both UPG and ALDG. The ALDG in these simulations is deployed based on empirically chosen ground-range trigger condition for PDI and initial value for time-to-go. The results illustrate that appropriate PDI condition and a right choice of time-to-go are very important in the performance and propellant usage of ALDG. Yet no existing approaches are available to effectively automate this process. We then proceed to develop a method dubbed UPG-augmented Apollo Powered Descent Guidance (UAPDG). In this approach, a feature of the UPG algorithm is used online to adaptively determine the PDI condition and time-to-go for ALDG, based on the actual flight condition. The ALDG then guides the vehicle to the landing site from the PDI point. Monte Carlo simulations of the same cases show UAPDG displays all the strengths of ALDG, and has a propellant performance very close to the optimum (that by UPG).

OVERVIEW OF UNIVERSAL POWERED GUIDANCE

The UPG algorithm finds the thrust direction, throttle setting, and burn time(s) in each guidance cycle based on the current state and targeting condition, while minimizing the propellant consumption. In contrast to Guidance for Fuel Optimal Large Divert (G-FOLD) in Refs. [6–8], UPG is based on the indirect method for optimal control, [1] meaning that UPG finds the guidance solution by meeting the necessary conditions in the optimal control theory as opposed to directly minimizing a cost function (fuel usage).

Optimal Powered Landing Problems

In a Cartesian coordinate system with the origin at the center of mass of the planet, the three-dimensional point-mass equations of motion for a rocket-powered vehicle can be written as

$$\dot{\boldsymbol{r}} = \boldsymbol{V} \tag{1}$$

$$\dot{\boldsymbol{V}} = \boldsymbol{g}(\boldsymbol{r}) + \frac{T}{m(t)}\mathbf{1}_T(t) \tag{2}$$

$$\dot{m} = -\frac{T}{v_{ex}} \tag{3}$$

The vectors $\boldsymbol{r} \in R^3$ and $\boldsymbol{V} \in R^3$ are the position and velocity vector of the vehicle with the current mass m. The gravitational acceleration $\boldsymbol{g}$ is a function of $\boldsymbol{r}$, and it has a magnitude of g_0 at the equatorial radius of the planet R_0. The rocket engine thrust has a magnitude T and $\mathbf{1}_T$ is the *unit* vector that defines the thrust direction which generally changes with time. T is allowed to vary as well, subject to a non-zero lower bound and an upper bound. Thus

$$T_{min} \leq T(t) \leq T_{max} \tag{4}$$

$$\|\mathbf{1}_T(t)\| = 1 \tag{5}$$

where $T_{min} > 0$ and $T_{max} > T_{min}$ are constant. The effective exhaust velocity of the rocket engine v_{ex} is also considered a constant. The initial state is assumed to be specified

$$\boldsymbol{r}(t_0) = \boldsymbol{r}_0, \quad \boldsymbol{V}(t_0) = \boldsymbol{V}_0, \quad m(t_0) = m_0 \tag{6}$$

The powered descent guidance problem is to determine the thrust magnitude profile $T(t)$ and the thrust direction $\mathbf{1}_T(t)$, subject to Eqs. (4) and (5), so that the trajectory of the vehicle will start from the current condition in Eq. (6) and end at a point where a set of prescribed terminal conditions is met

$$\boldsymbol{s}[\boldsymbol{r}(t_f), \boldsymbol{V}(t_f), t_f] = \mathbf{0} \tag{7}$$

The specific forms of the terminal constraints will be discussed shortly. An *optimal* powered descent guidance problem is a guidance problem as described above, plus the minimization of a performance index of the following form

$$J = \kappa\phi(\boldsymbol{r}_f, \boldsymbol{V}_f, t_f) + \int_{t_0}^{t_f} \frac{T}{v_{ex}} dt \tag{8}$$

where $\kappa \geq 0$ is a specified constant. Depending on the specific forms of the terminal constraints in Eq. (7) and the performance index in Eq. (8), three optimal powered descent problems can be solved in UPG. In all 3 variations of the optimal guidance problem to be defined below, the final time t_f in our problem setting is *free*, to be found as a part of the optimal solution.

Pinpoint Landing Problem Let $\boldsymbol{r}^* \in R^3$ be the specified vector that defines target position vector (e. g., the location of the landing site) and $\boldsymbol{V}^* \in R^3$ the vector that gives the target relative velocity with respect to the landing site. The terminal constraints in Eq. (7) in this problem take the specific form of

$$\boldsymbol{r}(t_f) = \boldsymbol{r}^* \tag{9}$$

$$\boldsymbol{V}(t_f) = \boldsymbol{V}^* \tag{10}$$

The performance index is just propellant consumption ($\kappa = 0$ in Eq. (8))

$$J_1 = \int_{t_0}^{t_f} \frac{T}{v_{ex}} dt \tag{11}$$

This problem requires that the vehicle uses the least amount of propellant to terminate its descent precisely at the target position with the required relative velocity, hence the *pinpoint landing* problem.

Bolza Landing Problem In this setting the vehicle is required to terminate at a specified altitude (or on the ground) with a specified relative velocity (vector). The terminal constraints are therefore now

$$\|\boldsymbol{r}(t_f)\| = \|\boldsymbol{r}^*\| \tag{12}$$

$$\boldsymbol{V}(t_f) = \boldsymbol{V}^* \tag{13}$$

where the 2-norm (Euclidean norm) is used in Eq. (12). The condition in Eq. (12) requires that the final planeto-centric altitude is equal to the prescribed value, but the landing location may be different from the

one specified by the vector $\boldsymbol{r}^*$. To put a penalty on the landing position error $\boldsymbol{r}(t_f) - \boldsymbol{r}^*$, the performance index is modified to be

$$J_2 = \kappa \left[\boldsymbol{r}(t_f) - \boldsymbol{r}^*\right]^T \left[\boldsymbol{r}(t_f) - \boldsymbol{r}^*\right] + \int_{t_0}^{t_f} \frac{T}{v_{ex}} dt, \quad \kappa > 0 \tag{14}$$

The Bolza landing problem aims at landing on the ground as closely as possible to the designated landing site without excessive propellant usage. The Bolza landing problem is likely to still have a solution in a case when the pinpoint-landing problem does not. This would happen when the divert requirement is beyond the capability of the vehicle, either due to large trajectory dispersions or contingencies such as partial failure of the retro-propulsion system.

Soft Landing Problem This problem has the same terminal constraints as in the Bolza landing problem

$$\|\boldsymbol{r}(t_f)\| = \|\boldsymbol{r}^*\| \tag{15}$$

$$\boldsymbol{V}(t_f) = \boldsymbol{V}^* \tag{16}$$

However the performance index is only propellant consumption (i. e., when $\kappa = 0$ in Eq. (14)):

$$J_3 = \int_{t_0}^{t_f} \frac{T}{v_{ex}} dt \tag{17}$$

In this problem the objective is to softly land on the ground with the minimum propellant usage, regardless of where the actual landing location is. There is no divert requirement to reach a specified location. The relationships among the 3 landing problems are investigated in Ref. [1] and the respective propellant usage is compared. For the same initial condition and specified $\boldsymbol{r}^*$ and $\boldsymbol{V}^*$, the soft-landing problem is the least numerically difficult, and the solution uses the least propellant among the 3 formulations. [1].

Method of Numerical Solution

It is theoretically established in Ref. [1] that in a constant-gravity field, the three-dimensional optimal descent problems formulated in the preceding section have the optimal thrust magnitude profile as shown in Fig. 1. The salient features of this profile which are all proved in Ref. [1] include (1) the bang-bang magnitude profile, (2) at most two switches of the optimal thrust magnitude between T_{max} and T_{min}, and (3) the particular sequence of switches from T_{max} to T_{min} and back to T_{max}, or a variation of this order, for instance, the full-throttle solution when $t_1 = t_2$ is optimal.

The application of the necessary conditions for the optimal control problem [9] leads to a two-point-boundary-value problem (TPBVP). When t_1 and t_2 are specified (cf. Fig. 1), this TPBVP can be cast into a system of 7 nonlinear algebraic equations

$$\boldsymbol{f}(\boldsymbol{z}) = \boldsymbol{0} \tag{18}$$

where $\boldsymbol{z} \in R^7$ is the 7 unknowns in the problem, one of which is the final time t_f. All of the equations in the system in Eq. (18) have closed-form expressions. Refer to Ref. [1] for details. A step-size-controlled Newton-Raphson method works effectively to solve the system in Eq. (18), well within a time threshold for real-time applications. Once $\boldsymbol{z}$ is found, the thrust vector direction $\boldsymbol{1}_T(t)$ is defined for all $t \in [t_0, t_f]$, and the current guidance command for thrust direction is $\boldsymbol{1}_T(t_0)$. The solution process is then repeated in the next guidance cycle with the actual state at the moment as the initial condition.

The theoretically optimal solution requires that the optimal values of t_1 and t_2 be found as a part of the solution. In Ref. [1] it was found that optimization of t_1 yielded little practically meaningful propellant usage improvement, when t_2 and t_f were optimized. Therefore in UPG t_1 is fixed at an appropriate value (e. g., 10 seconds). The optimal value of t_2 is found by an outer loop of univariate minimization by the Brent's method [10]. at the beginning of the powered descent. This loop is not called upon in subsequent guidance cycles because again no noticeable additional benefits are found by doing so.

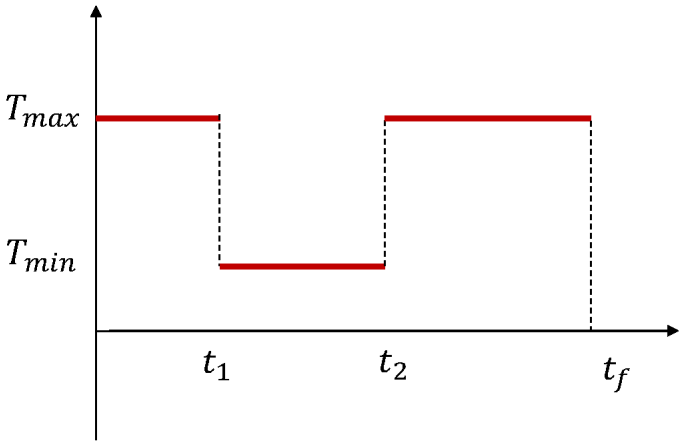

Figure 1. Propellant-optimal thrust magnitude profile

POWERED DESCENT INITIATION FOR UPG

The PDI point signifies the handover from entry to powered descent guidance. An adaptive PDI logic is developed and used in Refs. [1] and [2] to determine the PDI point for each dispersed trajectory based on the actual condition. While still in entry flight, this logic uses the soft-landing mode of UPG to solve the minimum-fuel soft-landing problem with current condition as the initial condition. The solution yields a predicted ground range should a fuel-optimal soft-landing trajectory be flown at the current time. When compared to the actual current range-to-go to the landing site, this predicted ground range will be an undershoot at first. As the vehicle flies closer and closer to the landing site (along the entry trajectory), this undershoot will eventually disappear and an overshoot will occur. As soon as the overshoot happens, the current condition is chosen to be the PDI point, and powered descent is commenced. Figure 2 illustrates this idea. More elaboration and application demonstration of this logic are in Refs. [1] and [2].

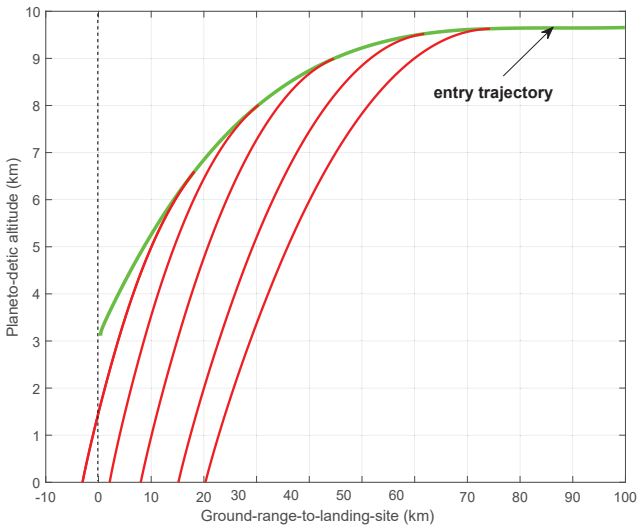

Figure 2. Illustration of the soft-landing trajectories along the entry flight path

Since the soft-landing trajectory is the one with the least propellant consumption among the 3 optimal powered landing problems, and no divert requirement, the PDI point so found is close to the best condition there can be along the entry trajectory, both in terms of incurring the least propellant usage and minimizing divert requirement for landing at the designated site. This logic determines automatically a very favorable PDI condition for each individual dispersed case based on the overall state condition in that case, rather than on a simplistic criterion of a single trigger parameter (altitude, velocity, time, and so forth).

APOLLO POWERED DESCENT GUIDANCE

Review of Apollo Lunar Descent Guidance

Apollo lunar descent guidance defines a thrust acceleration vector by a quadratic polynomial in time. In each guidance cycle and starting from the current condition, the coefficients of the thrust acceleration profile are found by meeting prescribed terminal values of the velocity, position, and thrust acceleration vectors. [3,4] When expressed in a feedback form, the ALDG law is

$$\boldsymbol{a}_T(t) = -\frac{6}{t_{go}}\left[\boldsymbol{V}^* - \boldsymbol{V}(t)\right] + \frac{12}{t_{go}^2}\left[\boldsymbol{r}^* - \boldsymbol{r}(t) - \boldsymbol{V}(t)t_{go}\right] + \boldsymbol{a}_f^* \tag{19}$$

where $\boldsymbol{a}_T = \boldsymbol{T}(t)/m(t)$, t_{go} is a specified time-to-go to the target condition, and $\boldsymbol{a}_f^*$ is a specified final thrust acceleration vector. By choosing the direction of $\boldsymbol{a}_f^*$ (for instance, in the local vertical direction), this feature of the ALDG law shapes the final part of the powered descent trajectory effectively. For this reason a terminal phase guidance by ALDG is integrated with UPG in Refs. [1] and [2] for a practically vertical final descent.

Note that the guidance law in Eq. (19) defines both the thrust magnitude and direction. But the upper and lower bounds of the thrust are not considered in designing the guidance law in Eq. (19). Hence, if the PDI condition is not well chosen, or it does not match t_{go}, saturation in the thrust magnitude will occur. If saturation is present in the last moment, the targeted final conditions $\boldsymbol{r}(t_f) = \boldsymbol{r}^*$ and $\boldsymbol{V}(t_f) = \boldsymbol{V}^*$ will not be met.

The other parameter t_{go} in Eq. (19) is also influential. A shorter t_{go} typically leads to less propellant consumption, everything else being equal. However, too short a t_{go} can cause the thrust to saturate on the upper bound (on the other hand too long a t_{go} can cause thrust saturation on the lower bound). In Ref. [4] an approach is discussed on finding t_{go} from solving for the roots of a cubic equation obtained by specifying the jerk component at the targeting point in the downrange direction. However, there is no reason that a t_{go} so generated will necessarily avoid thrust saturation. Furthermore, that approach appears only applicable to the case where the targeting condition is beyond the intended final point (so that the targeting point is never actually reached). In a fully autonomous powered descent mission where no terminal human piloted phase (as the one in Apollo Lunar Module descent) is planned, such a targeting strategy is not convenient.

BENCHMARKING THE POWERED DESCENT GUIDANCE ALGORITHMS

Simulation Setting

To evaluate and compare the performance of UPG and ALDG for a human Mars EDL mission, end-to-end closed-loop simulations in a three-degree-of-freedom simulation environment are carried out from the entry interface (EI) at an altitude of 129.18 km to touchdown at the designated landing site. The vehicle model is that of an aeroshell configuration called the mid lift-to-drag ratio Mars rigid vehicle (MRV). [5] Figure 3 shows the MRV in entry flight and powered descent. At the EI the MRV has a mass of 58000 kg. The hypersonic lift-to-drag ratio of the MRV is 0.58 with a ballistic coefficient of 397 kg/m^2. In its nominal configuration the MRV is fitted with a supersonic retro-propulsion (SRP) system with 8 engines, 4 mounted on each side. Each engine produces at full throttle a nominal thrust of 100,000 N, and has a specific impulse of 360 seconds. In the simulations in this paper it is assumed that the minimum throttle allowed is 25%.

In the entry phase the MRV is guided by the Fully Numerical Predictor-corrector Entry Guidance (FNPEG) algorithm. [11, 12] FNPEG is a fully automated and robust entry guidance algorithm applicable to vehicles

of a wide range of lift-to-drag ratios, and MRV is no exception. In Ref. [2] the significant effect of the entry trajectory on the propellant consumption in the powered descent phase is demonstrated, as well as how FNPEG can be set up to shape the entry trajectory in conjunction with the adaptive PDI logic for lowest propellant usage. The same approach is used here.

At the EI the vehicle's relative velocity is 4694 m/s. The downrange to the landing site is 1315 km. The entry flight is from south to north. The landing site is at the equator of Mars. The targeted touchdown condition is at zero planetodetic altitude with a descending rate of 1.0 m/s. A 3DOF trajectory is considered a success if the miss distance to the landing site is within 50 meters and the touchdown descent rate is no greater than 2.0 m/s.

In closed-loop 3DOF simulations in this paper FNPEG is called at 1 Hz. Only bank angle modulation is used for trajectory control, while the angle of attack is held at a trim value of 55 deg. The bank angle rate and acceleration are limited by 15 deg/s and 5 deg/s^2, respectively. For 6DOF simulation results on the MRV in the same mission with FNPEG, the reader is referred to Ref. [13]. During the powered descent, the guidance frequency is 5 Hz. For the MRV, the SRP engine thrust is assumed to be aligned with the body-normal axis (see Fig. 3). The direction of the thrust vector therefore defines the body frame. In powered descent simulations, the thrust vector direction (thus the vehicle body attitude) is defined in a 3-2-1 (yaw-pitch-roll) rotation sequence by the Euler angles with respect to the North-East-Down (NED) frame at the landing site. The pitch and yaw angles are subject to a rate limit of 15 deg/s in the simulations.

A total of 1000 cases are run in each scenario. The dispersions include those on the EI condition, lift and drag coefficients of the vehicle, and Martian atmosphere. The EI condition dispersions are generated by multiplying a covariance matrix to the position and velocity dispersions at the deorbit point. Each of the components of the position vector at the deorbit point is subject to a zero-mean Gaussian dispersion with a 3-sigma variation of 50 meters. Each of the component of the velocity vector at the deorbit point is subject to a zero-mean Gaussian dispersion with a 3-sigma variation of 0.5 m/s. The corresponding EI condition dispersions collected from the Monte Carlo simulations are summarized in Table 1 below. The dispersed atmospheric density profiles are generated by the Mars Global Reference Atmospheric Model (Mars GRAM 2010) [14] which generates random atmospheric density dispersions dependent on a number of parameters including altitude, location, time, and others. A parameter in Mars GRAM 2010 is *dusttau* that specifies the optical depth of background dust level which affects the atmospheric density as well. The value of *dusttau* is dispersed uniformly between 0.1 and 0.9 in our simulations. The dispersions in C_L and C_D are zero-mean Gaussian noise with a 3-sigma variations of 10%. On the other hand, perfect navigation information is assumed in this paper.

Table 1. Dispersions for Monte Carlo Simulations

	standard deviation	maximum/3σ	minimum/-3σ
EI velocity (m/s)	1.27E-01	3.57E-01	-4.07E-01
EI flight-path angle (deg)	7.26E-03	2.05E-02	-2.39E-02
EI ground range (km)	1.09E+01	3.5E+01	-3.5E+01
EI crossrange (km)	9.73E+00	2.61E+01	-3.27E+01
C_L	3.33%	10%	-10%
C_D	3.33%	10%	-10%
atmospheric density	Mars GRAM 2010	Mars GRAM 2010	Mars GRAM 2010
dusttau	uniform distribution	0.9	0.1

Performance Comparison

Henceforth in this section, when we refer to UPG in presenting and discussing simulation results, it is meant to be UPG plus a terminal phase guidance with ALDG, as explained in Ref. [2] and the section reviewing

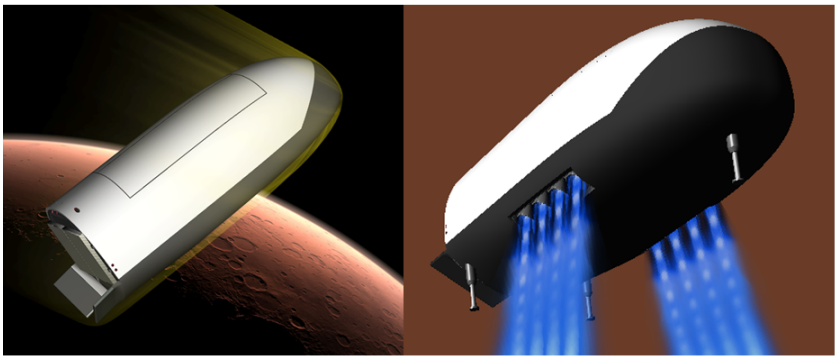

Figure 3. Mid L/D rigid vehicle for human Mars missions in entry flight and powered descent

ALDG. If no terminal phase with Apollo guidance is present when UPG is used, it will be called "pure UPG".

The simulations stopped either when the time-to-go was zero or the planetodetic altitude became zero or negative. The statistics of the touchdown conditions under UPG and pure UPG are summarized in Tables 2 and 3. While not shown in the tables, it should be mentioned that the optimal throttle-back phase under UPG and pure UPG turns out to have a zero duration (i. e., $t_1 = t_2$ in Fig. 1). The landing accuracy in Table 2 is determined by the ALDG, as a terminal phase by ALDG is used before touchdown. The miss distances are at the level of centimeters (recall that perfect navigation is assumed). The accuracy in Table 3 is produced by the UPG algorithm because no terminal phase is present. The miss distances in this case are in meters. In both cases the touchdown accuracy is very good. The propellant consumptions differ. On average, the propellant penalty for including a terminal phase guided by ALDG versus using only the fuel-optimal UPG is 470 kg. However, this may be a small price to pay, given the high accuracy of ALDG and the desirable vertical trajectory before touchdown. [1]

Table 2. Statistics of final conditions at touchdown under UPG

	mean	standard deviation	maximum	minimum
miss (m)	3.41E-02	1.77E-03	3.83E-02	2.95E-02
altitude (m)	2.47E-02	4.33E-04	2.58E-02	2.24E-02
descending rate (m/s)	1.12E+00	3.38E-03	1.14E+00	1.11E+00
flight path angle (deg)	-7.90E+01	4.23E-01	-7.79E+01	-8.01E+01
propellant usage (kg)	**8.65E+03**	1.81E+02	9.30E+03	8.07E+03
powered descent flight time (s)	4.21E+01	9.03E-01	4.53E+01	3.91E+01

Next, for the same mission ADLG is employed for powered descent. For ALDG, the PDI point and the

Table 3. Statistics of final conditions at touchdown under pure UPG

	mean	standard deviation	maximum	minimum
miss (m)	4.47E+00	2.00E+00	1.98E+01	5.05E-02
altitude (m)	3.18E-04	5.46E-03	6.44E-02	-3.49E-03
descending rate (m/s)	1.01E+00	1.94E-02	1.02E+00	7.77E-01
flight path angle (deg)	-8.92E+01	3.30E-01	-8.43E+01	-8.99E+01
propellant usage (kg)	**8.18E+03**	1.76E+02	8.77E+03	7.65E+03
powered descent flight time (s)	3.61E+01	7.75E-01	3.87E+01	3.38E+01

initial value of the time-to-go must be specified in some way. In this benchmark evaluation, we tested many possibilities, by trial and error. Table 4 lists the statistics of the final conditions for 3 scenarios. In each scenario, the PDI is triggered by a specific value of the ground range to the landing site. The time-to-go at PDI (the initial value of t_{go}) is also prescribed by a chosen value that seems reasonable. After that, the time-to-go is simply calculated by subtracting the time elapsed since PDI from this initial time-to-go. It is clear that in the first two scenarios, ALDG is successful in steering all the cases to the landing site with high accuracy. The first two scenarios also suggest that a shorter trigger ground range and smaller initial t_{go} will render less propellant consumption. However, continuing to push in this direction with shorter ground range trigger and t_{go} risks the breakdown of guidance performance, as shown in the 3rd scenario in Table 4. In this scenario quite some cases failed to achieve the required landing condition, in miss distance, final descending rate, and final altitude. Indeed, Figs. 4 and 5 show the scatter of the final positions and the final altitude versus final descent velocity (descending rate) for each of the 1000 trajectories in the 3rd scenario. Quite many cases had miss distances of several hundred meters, and most of these ended with terminal velocities of tens of meters per second and at altitudes of tens of meters. All these failed cases were caused by thrust magnitude saturation, an unmistakable indication that the PDI condition was not appropriate. For any particular entry trajectory, a good PDI ground range trigger value and t_{go} can always be found by trial and error so that a as small as possible propellant consumption in powered descent is achieved. The difficulty is that these selections do not work for all other dispersed entry trajectories.

Table 4. Final condition statistics under Apollo lunar descent guidance

PDI conditions	parameter	mean	stdev	max	min
range=20 km $t_{go} = 100$ s	miss (m)	2.97E-03	1.03E-04	3.32E-03	2.65E-03
	h_f (m)	2.29E-02	5.84E-05	2.31E-02	2.27E-02
	descending rate (m/s)	1.11E+00	3.52E-04	1.11E+00	1.11E+00
	fuel usage (kg)	**1.12E+04**	1.55E+02	1.17E+04	1.06E+04
range=15 km $t_{go} = 75$ s	miss (m)	5.89E-03	1.82E-04	6.54E-03	5.27E-03
	h_f (m)	2.21E-02	1.08E-04	2.25E-02	2.18E-02
	descending rate (m/s)	1.12E+00	6.40E-04	1.12E+00	1.12E+00
	fuel usage (kg)	**1.00E+04**	1.46E+02	1.06E+04	9.56E+03
range=10 km $t_{go} = 50$ s	miss (m)	1.72E+01	6.46E+01	4.24E+02	3.37E-04
	h_f (m)	3.54E+00	1.25E+01	8.80E+01	-3.63E-01
	descending rate (m/s)	7.19E+00	2.07E+01	1.27E+02	1.13E+00
	fuel usage (kg)	9.01E+03	3.53E+02	1.08E+04	7.28E+03

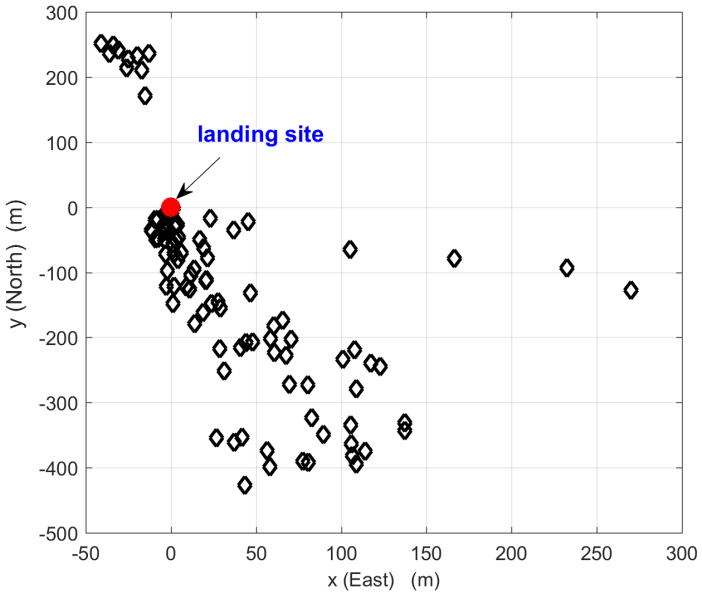

Figure 4. Final positions of the powered descent trajectories under ALDG with PDI ground range of 10 km, and $t_{go} = 50$ s

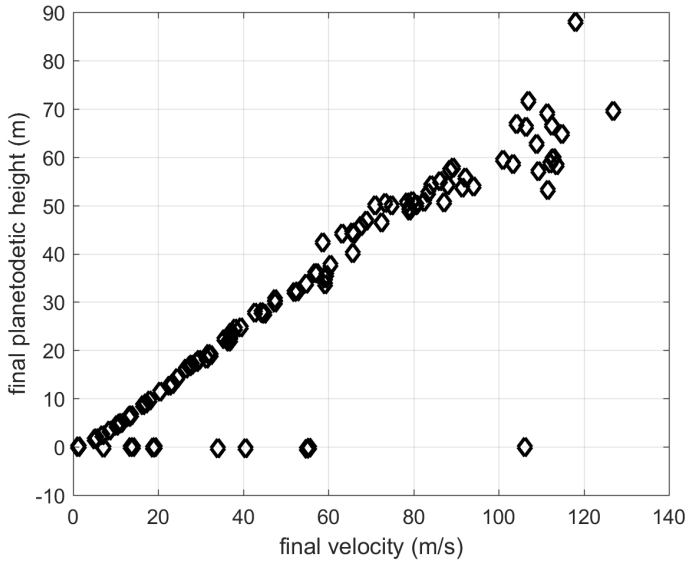

Figure 5. Final altitudes vs final descending rates of the powered descent trajectories under ALDG with PDI ground range of 10 km, and $t_{go} = 50$ s

UPG-AUGMENTED APOLLO POWERED DESCENT GUIDANCE

Approach

The simulation results seen in the preceding section clearly demonstrate how important a good PDI condition and the choice of time-to-go are for the performance and propellant consumption. While for a specific vehicle and a particular mission it may be possible to determine by trial and error a reasonable PDI trigger based on a parameter (like ground range) and a time-to-go, it is laborious and completely ad hoc. For each dispersed trajectory, such fixed simple PDI trigger and time-to-go are generally not the best there can be. And to be applicable to all expected dispersed cases, inherently the one-size-fits-all choices like these will have to be conservative.

In light of how UPG finds its PDI condition in each individual case, a natural question to ask is: can the same adaptive PDI logic be used to determine the PDI condition for ALDG? The answer is yes, with a caveat. Recall that the UPG adaptive PDI logic is based on a predicted soft-landing trajectory. This solution uses the 3-arc optimal thrust magnitude profile in Fig. 1. The optimal solution could be such that $t_2 = t_1$, i. e., the throttle-back phase vanishes. Indeed, when the entry trajectory is shaped for best propellant performance (see Ref. [2]), the soft-landing solution that triggers PDI has for most cases exactly this feature - a zero duration for the throttle-back arc. As a result, the actual trajectory to land softly at the designated site most likely will demand full thrust. In such a case, the found PDI point will not be appropriate for ALDG. This is because the ALDG law will saturate the engine starting at such a condition.

The remedy is actually exceedingly simple. In the UPG code, bounds can be set on all parameters to be solved. Setting a non-zero bound on the minimum of $t_2 - t_1$ in the algorithm will ensure that the throttle-back arc has a non-zero duration in any UPG solution, including the soft-landing solution. Hence the PDI condition will be one from which powered descent to touchdown at the landing site is achievable by a trajectory with the thrust on the lower bound for some time. In other words, from a standpoint of impulse imparted by the thrust, there should be a feasible trajectory from the PDI point to the landing site with a (mean) thrust magnitude less than its upper bound. The larger this lower bound on $t_2 - t_1$ is, the smaller this mean thrust will be, which in turn makes it less likely that the Apollo powered guidance will saturate the engine at the maximum thrust from such a PDI condition. For MRV, a constraint of $t_2 - t_1 \geq 5$ s appears sufficient to prevent the ALDG law from saturating thrust and resulting large terminal errors.

Finally, recall that the soft-landing solution by UPG includes the time of flight, denoted by t_{UPG}. This value provides a basis for the time-to-go t_{go} used in the ALDG law in Eq. (19). Since t_{UPG} is for a soft-landing solution that has no divert requirement, and the actual trajectory will need to maneuver to land at the designated site, the actual time-to-go should be allowed some margin. The following empirical rule appears to work well

$$t_{go} = 1.2 t_{UPG} \tag{20}$$

Let us re-cap the powered descent guidance approach just outlined above. The UPG adaptive PDI logic as developed in Ref. [1] is amended with a non-zero lower bound on the throttle-back phase. Otherwise the same logic is employed to check and determine the PDI condition along the entry trajectory, based on the actual condition. Once the powered descent phase is commenced, the guidance is performed by the Apollo lunar descent guidance law, with the initial value of t_{go} defined by Eq. 20, where t_{UPG} is the time of flight of the soft-landing solution that triggered the PDI. The values of t_{go} in the subsequent guidance cycles are from subtracting the time elapsed since PDI from this initial t_{go}. We will call this hybrid approach UPG-augmented Apollo Powered Descent Guidance (UAPDG).

Evaluation

The same mission used in the benchmark testing is taken on again with Apollo powered descent guidance for powered descent, only this time the PDI condition is determined by the UPG PDI logic (with a constraint $t_2 - t_1 \geq 5$ s). Figures 6–8 depict the nominal powered descent trajectory under UAPDG. The nominal used 9,130 kg propellant. The PDI point determined by the UPG logic is at a ground range of 11,626 m to the landing site, altitude of 2,784 m, and relative velocity of 514.1 m/s (Mach 2.28). The nominal powered

descent time was 50.83 s. From Fig. 7 the nominal throttle is not saturated at either the upper or lower bound anywhere. The benign pitch and yaw angle profiles (with respect to the NED frame at the landing site) in Fig. 8 suggest a rather small divert requirement along the nominal trajectory. In fact the yaw angle is practically constant, meaning that the powered descent trajectory is nearly planar. This is not necessarily the case if the PDI condition is determined by a fixed value of ground range (or other similar simple triggers). More will be discussed on this below. Also, note that the final pitch angle is close to zero, indicating a nearly horizontal touchdown as desired (cf. Fig. 3).

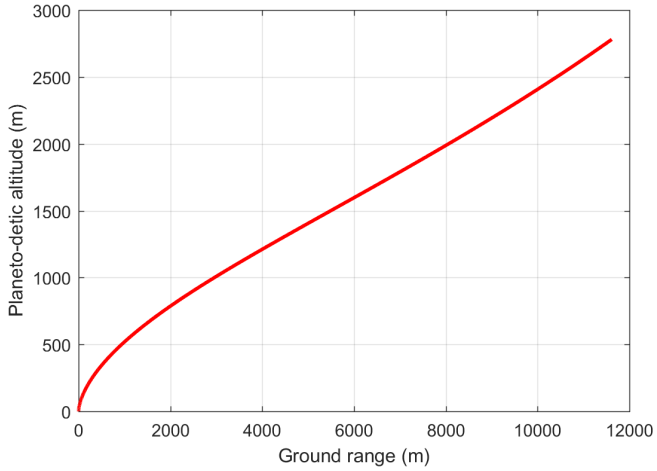

Figure 6. Nominal altitude versus ground range during the powered descent guided by UAPDG

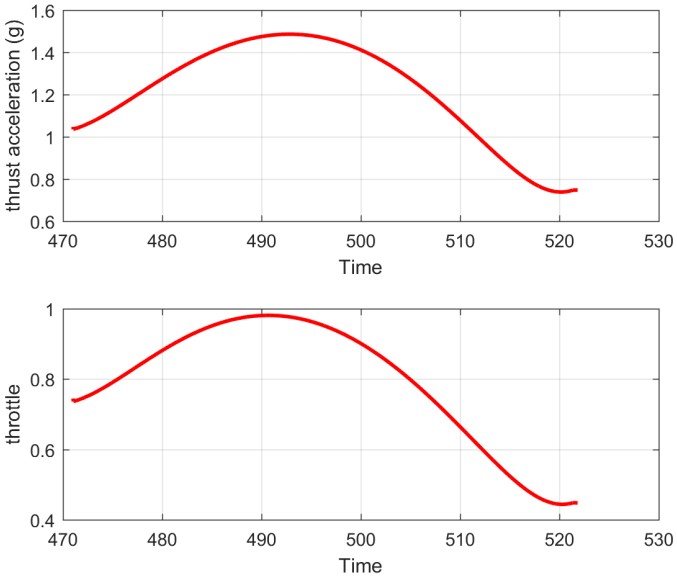

Figure 7. Nominal thrust acceleration (in Earth g) and engine throttle during the powered descent guided by UAPDG

Next the same 1000 dispersed cases were run with UAPDG. The statistics of the touchdown conditions under this UAPDG approach are given in Table 5. The statistics of the PDI conditions are summarized in

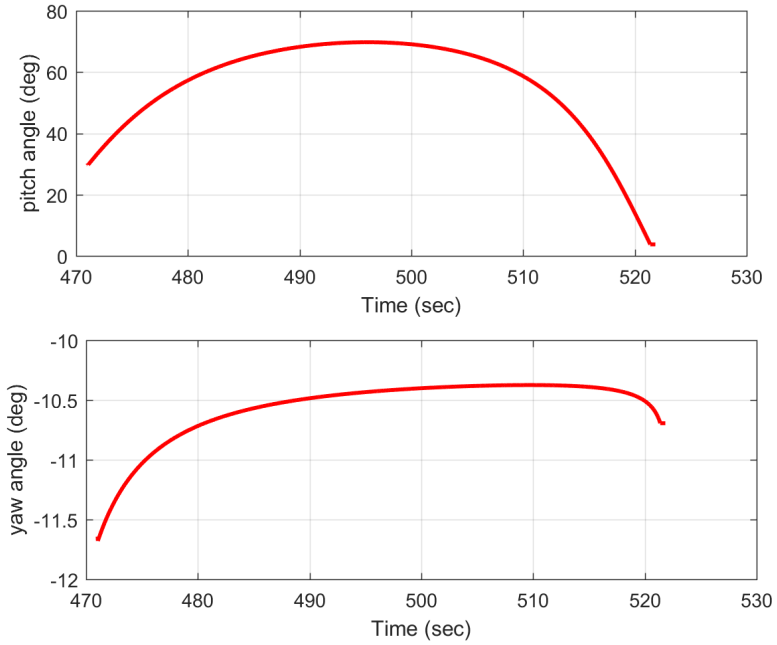

Figure 8. Nominal Euler angle profiles during the powered descent guided by UAPDG

Table 6. From these two tables it can be seen that the average time of flight for powered descent was 50.5 s, and the average ground range at PDI was 11.3 km. These values are quite close to those in the 3rd scenario in Table. 4. However, unlike the many failed cases in the 3rd scenario in Table. 4, all 1000 dispersed cases were a perfect success this time around. The difference is solely attributable to the PDI logic in UAPDG which finds a favorable PDI point based on the complete trajectory state for *each* case, as opposed to a simple one-size-fits-all trigger on a particular state or parameter.

With UAPDG, not only is high targeting performance reliably achieved, but also nearly optimal is the propellant performance. Comparing the average and maximum propellant usages in Table 5 with those in Table 2, we see that the difference in propellant consumption of UAPDG is only 400 kg more than that of UPG (plus a terminal phase guided by ALDG), for a vehicle of 58,000 kg at EI. Even compared to the propellant performance of pure UPG in Table 3, the difference in average fuel usage is just 800 kg. Figure 9 shows the distribution of the propellant consumption among the dispersed cases under UAPDG.

One interesting observation on Table 6 is that the crossranges with respect to the landing site at PDI were all practically zero. The same phenomenon was noticed using UPG in Refs. [1] and [2]. Although a zero crossrange is not a criterion used when the PDI logic based on the soft-landing mode of UPG searches for the PDI point, it appears in the cases we have tested that such a point always occurs at a condition with near zero crossrange (the reverse is not true, namely, a point with zero crossrange is not necessarily the PDI condition sought). An immediate benefit of this feature is that the powered descent trajectory will have little out-of-plane divert requirement, and the powered descent trajectory is basically planar. This is confirmed by the nearly constant yaw angle in Fig. 8.

Table 5. Statistics of touchdown conditions under UPG-augmented Apollo Powered Descent Guidance

	mean	standard deviation	maximum	minimum
miss (m)	1.68E-02	8.08E-04	1.87E-02	1.47E-02
altitude (m)	2.47E-02	4.33E-04	2.58E-02	2.24E-02
descending rate (m/s)	1.12E+00	2.18E-03	1.13E+00	1.11E+00
flight path angle (deg)	-8.46E+01	1.81E-01	-8.41E+01	-8.51E+01
propellant usage (kg)	**9.06E+03**	1.95E+02	9.76E+03	8.44E+03
powered descent flight time (s)	5.05E+01	9.92E-01	5.41E+01	4.74E+01

Table 6. Statistics of PDI conditions for UPG-augmented Apollo Powered Descent Guidance

	mean	standard deviation	maximum	minimum
ground range (m)	1.13E+04	4.78E+02	1.31E+04	9.78E+03
crossrange (m)	2.12E-08	1.24E-08	6.80E-08	-2.66E-08
altitude (m)	2.93E+03	2.41E+02	3.76E+03	2.08E+03
velocity (m/s)	5.06E+02	1.21E+01	5.49E+02	4.66E+02
time since EI (s)	4.79E+02	8.67E+00	5.04E+02	4.51E+02

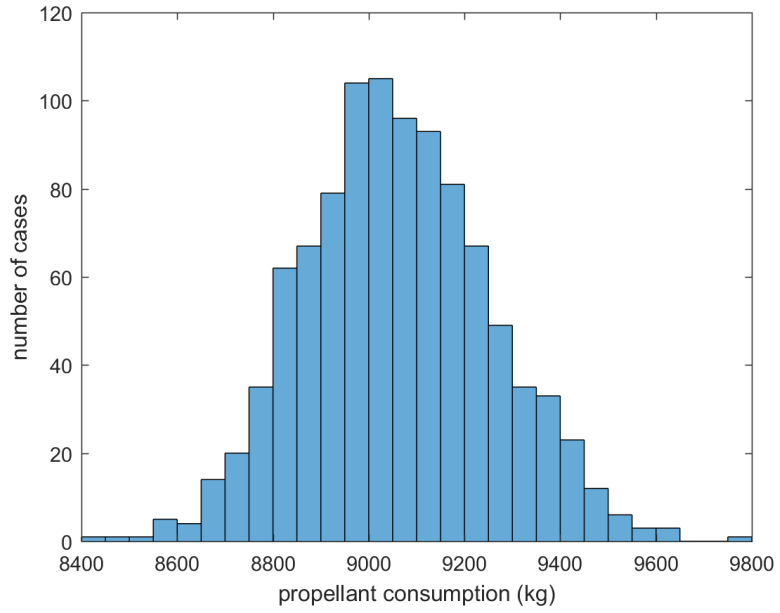

Figure 9. Propellant consumptions of dispersed powered descent trajectories guided by UAPDG

CONCLUSIONS

In this paper a fuel-optimal powered descent guidance algorithm (dubbed Universal Powered Guidance (UPG)) and the Apollo lunar descent guidance (ALDG) are evaluated side by side for a human Mars mission in closed-loop end-to-end simulations from entry to touchdown. UPG is fully autonomous in that it determines online when to start the powered descent along the entry trajectory, and how to minimize fuel consumption in powered descent. The performance of ALDG, in both landing precision and propellant consumption, is greatly affected by the powered descent initiation (PDI) condition and time-to-go. However, previously there did not exist a systematic and effective technique to automate the determination of the PDI condition and time-to-go for ALDG. In this work the soft-landing solution mode of UPG provides a novel answer to such a need. This capability of UPG will find on the basis of the actual condition a favorable PDI condition and help generate an appropriate time-to-go for ALDG to achieve the specified landing condition without excessive propellant usage. This UPG-augmented Apollo powered descent guidance approach proves to preserve the characteristic high landing precision of ALDG, yet offers a propellant-usage performance reliably close to the optimal. This development removes two long-standing issues in applying ALDG (ensured landing performance and fuel optimality). Given the simplicity, robustness, and flight-proven heritage of the ALDG, this UPG-augmented Apollo powered descent guidance method should be a strong contender for a future human Mars mission.

Acknowledgments

This research has been supported by NASA Cooperative Agreement NNX16AL35A. Technical exchanges with Christopher Cerimele and Ronald Sostaric of NASA Johnson Space Center are appreciated.

REFERENCES

[1] Lu, P., "Propellant-Optimal Powered Descent Guidance," *Journal of Guidance, Control, and Dynamics*, 2017, available online.
doi:10.2514/1.G003243.

[2] Lu, P., Sostaric, R., and Mendeck, G., "Adaptive Powered Descent Initiation and Fuel-Optimal Guidance for Mars Applications," AIAA Paper 2018-0616, January, 2018.

[3] Cherry, G. W., "A General, Explicit, Optimizing Guidance Law for Rocket-Propelled Spaceflight," AIAA Paper 64-638, 1964.
doi:10.2514/6.1964-638.

[4] Klumpp, A. R., "Apollo Lunar Descent Guidance," *Automatica*, Vol. 10, No. 3, 1975, pp. 133–146.
doi:10.2514/3.3060.

[5] Cerimele, C., Robertson, E., Sostaric, R., Campbell, C., Robinson, P., Matz, D., Johnson, B., and Stachowiak, S., "A Rigid Mid Lift-to-Drag Ratio Approach to Human Mars Entry, Descent, and Landing," AIAA Paper 2017-1898, 2017.
doi:10.2514/6.2017-1898.

[6] Acikmese, B. and Ploen, S. R., "Convex Programming Approach to Powered Descent Guidance for Mars Landing," *Journal of Guidance, Control, and Dynamics*, Vol. 30, No. 5, 2007, pp. 1353–1366.
doi:10.2514/1.27553.

[7] Blackmore, L., Acikmese, B., and Scharf, D. P., "Minimum Landing Error Powered Descent Guidance for Mars Landing Using Convex Optimization," *Journal of Guidance, Control, and Dynamics*, Vol. 33, No. 4, 2010, pp. 1161–1171.
doi:10.2514/1.47202.

[8] Acikmese, B., Carson, J., and Blackmore, L., "Lossless Convexification of Nonconvex Control Bound and Pointing Constraints of the Soft Landing Optimal Control Problem," *IEEE Transactions on Control Systems Technology*, Vol. 21, No. 6, 2013, pp. 2104–2113.
doi:10.1109/TCST.2012.2237346.

[9] Pontryagin, L. S., Boltyanskii, V. G., Gramkreledze, Q. V., and Mishchenko, E. F., *The Mathematical Theory of Optimal Processes*, Intersciences, New York, 1962, pp. 20–21,311–316.

[10] Brent, R., *Algorithms for Minimization without Derivatives*, chap. 4,5, Prentice-Hall, Englewood Cliffs, NJ, 1973.

[11] Lu, P., "Entry Guidance: a Unified Method," *Journal of Guidance, Control, and Dynamics*, Vol. 37, No. 3, 2014, pp. 713–728.
doi:10.2514/1.62605.

[12] Lu, P., Brunner, C., Stachowiak, S., Mendeck, G., Tigges, M., and Cerimele, C., "Verification of a Fully Numerical Entry Guidance Algorithm," *Journal of Guidance, Control, and Dynamics*, Vol. 40, No. 2, 2017, pp. 230–247.
doi:10.2514/1.G000327.

[13] Johnson, B., Cerimele, C., Stachowiak, S., Sostaric, R., and Matz, D., "Mid-Lift-to-Drag Ratio Rigid Vehicle Control System Design and Simulation for Human Mars Entry," AIAA Paper 2018-0615, January, 2018.

[14] Justh, H. L., *Mars Global Reference Atmospheric Model 2010 Version: Users Guide*, NASA/TM-2014-217499, 2014.